ANALYSIS OF WHOLE GENOME SEQUENCING IN A COHORT OF INDIVIDUALS WITH PHACE SYNDROME SUGGESTS DYSREGULATION OF RAS/PI3K SIGNALING

Short title: WHOLE GENOME SEQUENCING ANALYSIS IN PHACE SYNDROME

Authors: Elizabeth S. Partan (1,2), Francine Blei (3), Sarah L. Chamlin (4,5,6), Olivia M. T. Davies (7), Beth A. Drolet (8), Ilona J. Frieden (9,10), Ioannis Karakikes (11), Chien-Wei Lin (12), Anthony J. Mancini (4,5,6), Denise Metry (13), Anthony Oro (14), Nicole S. Stefanko (4), Laksshman Sundaram (15), Monika Tutaj (16), Alexander E. Urban (17,18), Kevin C. Wang (14, 19), Xiaowei Zhu (17,18), Nara Sobreira* (1, 20), Dawn H. Siegel* (21)

Affiliations

1. McKusick-Nathans Department of Genetic Medicine, Johns Hopkins Medicine, Baltimore, MD
2. Predoctoral Training Program in Human Genetics, Johns Hopkins School of Medicine, Baltimore, MD
3. Department of Pediatrics / Vascular Anomalies Program, NYU Langone Health, Grossman School of Medicine, New York, NY
4. Department of Dermatology, Northwestern University Feinberg School of Medicine, Chicago, IL
5. Department of Pediatrics, Northwestern University Feinberg School of Medicine, Chicago, IL
6. Division of Dermatology, Ann & Robert H. Lurie Children's Hospital of Chicago, Chicago, IL

7. Medical College of Wisconsin, Milwaukee, WI
8. Department of Dermatology, University of Wisconsin School of Medicine and Public Health, Madison, WI
9. Department of Dermatology, University of California San Francisco, San Francisco, CA
10. Department of Pediatrics, University of California San Francisco, San Francisco, CA
11. Department of Cardiothoracic Surgery, Stanford University, Palo Alto, CA
12. Division of Biostatistics, Institute for Health and Equity, Medical College of Wisconsin, Milwaukee, WI
13. Department of Dermatology, Baylor College of Medicine, Houston, TX
14. Department of Dermatology, Stanford University, Palo Alto, CA
15. Department of Computer Science, Stanford School of Engineering, Palo Alto, CA
16. Department of Biomedical Engineering, Medical College of Wisconsin, Milwaukee, WI
17. Department of Psychiatry and Behavioral Sciences, Stanford University, Palo Alto, CA
18. Department of Genetics, Stanford University, Palo Alto, CA
19. Veterans Affairs Healthcare System, Palo Alto, CA
20. Department of Pediatrics, Johns Hopkins Medicine, Baltimore, MD
21. Department of Dermatology, Medical College of Wisconsin, Milwaukee, WI

* These authors contributed equally to this work

Work was performed in Baltimore, MD, USA; Milwaukee, WI, USA; and Palo Alto, CA, USA

Corresponding author: Dawn Siegel • 414-955-2818 • dsiegel4@stanford.edu

Abbreviations used: single nucleotide variant (SNV), copy number variant (CNV), extracellular matrix (ECM)

ABSTRACT

The acronym PHACE stands for the co-occurrence of posterior brain fossa malformations, hemangiomas, arterial anomalies, cardiac defects, and eye abnormalities. The majority of patients have a segmental hemangioma and at least one developmental structural anomaly. The etiology and pathogenesis are unknown. Here we discuss the candidate causative genes identified in a *de novo* analysis of whole genome sequencing of germline samples from 98 unrelated trios in which the probands had PHACE, all sequenced as part of the Gabriella Miller Kids First Pediatric Research Program. A g:Profiler pathway analysis of the genes with rare, *de novo* variants suggested dysregulation of the RAS/MAPK and PI3K/AKT pathways that regulate cell growth, migration, and angiogenesis. These findings, along with the developmental anomalies and the vascular birthmark, support including PHACE within the RASopathy family of syndromes.

INTRODUCTION

The RASopathies represent a collection of rare genetic conditions caused by mutations in individual genes within the RAS/MAP kinase (MAPK) pathway. RAS/MAPK signaling is upstream of many cellular pathways; therefore, depending on the individual mutation and affected tissue, single-gene perturbations can cause numerous syndromes, including Cardio-Facio-Cutaneous (CFC), Costello (CS), Legius (LS), Neurofibromatosis type 1 (NF1), Noonan (NS), Noonan-like (NS with Multiple Lentigines, NSML; NS with Loose Anagen Hair, NSLH) and Capillary Malformation-Arteriovenous Malformation (CM-AVM) (Grant et al. 2018; Stevenson et al. 2016). These syndromes share many clinical features including distinct facial features, developmental delays,

cardiac defects, growth delays, and structural brain anomalies. While these individual syndromes are rare, as a group the RASopathies are among the most common genetic conditions in the world. The vast majority of mosaic neurocutaneous syndromes have been shown to be caused by somatic variants in RAS pathway genes, including the association of *HRAS* and *KRAS* variants with sebaceous nevus syndrome and *NRAS* variants with neurocutaneous melanosis (Chacon□Camacho et al. 2019; Kinsler et al. 2013).

The PHACE (OMIM 606519) acronym represents the sporadic vascular syndrome exhibiting the co-occurrence of posterior brain fossa malformations, hemangiomas, arterial anomalies, cardiac defects, and eye abnormalities (Frieden et al. 1996). The majority of patients have a segmental infantile hemangioma and at least one other feature (Garzon et al. 2016; Metry et al. 2009). Dysplasia and stenosis of the arteries of the head and neck is the second most common feature (occurring in >85%), followed by structural brain anomalies (including hypoplastic cerebellum), cardiovascular anomalies (including aortic coarctation or ventricular septal defect), and eye anomalies (Metry et al. 2009; Siegel 2017). The significant overlap in developmental anomaly phenotypes between PHACE and RASopathy patients suggests a common mechanistic underpinning of sporadic PHACE and germline RASopathy variants (Ruggieri et al. 2020).

The etiology and pathogenesis of PHACE are unknown, although consideration of the variety of body systems affected suggests that the age of onset is between 3 and 12 weeks of gestation during early vasculogenesis (Frieden et al. 1996; Metry et al. 2006; Siegel 2017). There is a 6:1 female:male preponderance, but no significant difference in the severity of the phenotype between males and females (Metry et al. 2009; Wan et al. 2017). PHACE is a sporadic disorder; there are no reported familial cases and at least four female patients with PHACE have given birth to clinically unaffected children (Martel et al. 2015; Stefanko et al. 2019). PHACE

is believed to have a genetic cause because there is no evidence of a common exposure during gestation or early infancy for children diagnosed with PHACE (Wan et al. 2017). Autosomal dominant inheritance caused by *de novo*, germline pathogenic variants or mosaicism caused by somatic mosaic pathogenic variants have been suggested as possible modes of inheritance (Mitchell et al. 2012; Siegel 2017).

Here we present the *de novo* analysis of whole genome sequencing (WGS) of germline samples from 98 unrelated trios in which the probands had PHACE, all sequenced as part of the Gabriella Miller Kids First project (X01HL140519-01). Additionally, we analyzed the DECIPHER database (Firth et al. 2009) for genes affected by copy number variants (CNVs) identified in individuals with the search terms "hemangioma" and "facial hemangioma" and used this analysis to prioritize genes with *de novo* variants identified among our cohort of 98 patients. Among the rare, *de novo* variants, we prioritized variants in 10 genes in 18 patients; six of these genes were in the RAS pathway. Our results support including PHACE within the RASopathy family of syndromes.

RESULTS

Germline whole genome sequencing and *de novo* analysis pipeline

We identified a total of 16,107 *de novo* single nucleotide variants (SNVs) in our cohort of 98 patients; on average, this is 164 SNVs per patient. Our analysis found 15,752 rare (minor allele frequency [MAF] < 1%), *de novo* variants, including 219 coding variants (119 missense/nonsense/stoploss/splicing and 100 synonymous) and 15,533 noncoding variants. No *de novo* variant was found in more than two patients, and no gene had nonsynonymous, *de novo* coding variants in more than one patient.

Variant prioritization

Among the rare, *de novo* variants, we prioritized 18 candidate SNVs in 10 genes in 18 patients, and two indels in these same genes (Supplemental Table 1; see Methods for a description of prioritization metrics). Briefly, variants were prioritized if they were rare or novel (population frequency < 1% or 0), affected a gene known to cause a phenotype similar to PHACE in humans or mice, or affected genes disrupted by CNVs in a previous study of PHACE (Siegel et al. 2013).

Genes associated with vascular human phenotypes

Using OMIM annotation, we identified a missense, heterozygous *STAMBP*–p.Ile301Asn variant in Patient 16. Missense and frameshift homozygous or compound heterozygous variants in this gene cause autosomal recessive microcephaly-capillary malformation syndrome (OMIM 614261), which is characterized by capillary malformation, microcephaly, optic atrophy, cleft palate, tapered fingers, and seizures. *STAMBP*–p.Ile301Asn is not found in gnomAD and is predicted to be pathogenic by 18 *in silico* algorithms. Additionally, 88% of non-VUS missense variants in this gene are pathogenic. Patient 16 was heterozygous for the *STAMBP*–p.Ile301Asn variant and a second candidate variant in this gene was not identified despite careful analysis of the WGS data including a search for deletions or duplications.

Genes associated with vascular mouse phenotypes

We then identified coding and noncoding variants in six genes associated with lethal knockout mouse models due to vascular abnormalities. Two variants, *RASA3*–p.Val85Met in Patient 4 and *THBS2*–p.Asp859Asn in Patient 14, were exonic. The *RASA3*–p.Val85Met variant is predicted to be pathogenic by 11 algorithms (CADD, DEOGEN2, EIGEN, FATHMM-MKL, FATHMM-XF,

LRT, Mutation assessor, MutationTaster, PrimateAI, SIFT, and SIFT4G) and to affect splicing. The *THBS2*–p.Asp859Asn variant is found in the C-terminal type 3 repeats and likely disrupts intraprotein interactions and calcium binding (Figure 1); this variant is predicted to be pathogenic by 19 algorithms (BayesDel-addAF, BayesDel-noAF, CADD, DEOGEN2, EIGEN, EIGEN PC, FATHMM, FATHMM-MKL, FATHMM-XF, LIST-S2, MVP, MetaLR, MetaSVM, Mutation assessor, MutationTaster, PROVEAN, REVEL, SIFT, and SIFT4G). The other variants were noncoding and included two intronic SNVs in *BCAS3*, three intronic SNVs in *DLC1*, one intronic SNV in *GLRX3*, one intronic SNV in *PIK3CA*, and one intronic SNV in *THBS2* (see Supplemental Table 1). Most of the identified variants are novel. Variants in *BCAS3*, *DLC1*, *GLRX3*, and *PIK3CA* are predicted to affect splicing. Variants in *BCAS3*, *DLC1*, *PIK3CA*, and *THBS2* are predicted to be pathogenic by at least one algorithm. The *BCAS3* SNV in intron 23 is predicted to fall within a binding site for GATA1 and the *THBS2* intronic SNV is predicted to fall in a binding site for IKZF1. All three variants in *DLC1* and the variants in *GLRX3* and *PIK3CA* are predicted to be in open chromatin in human vascular endothelial cells (HUVECs) by Encode and therefore accessible to proteins regulating gene expression: four are predicted to be transcribed, and one (*DLC1* intron 5) is predicted to be in an enhancer.

Genes previously implicated in CNV analysis

We next looked for variants in genes affected by CNVs identified in a cohort of patients with PHACE described by Siegel et al. (2013) among our cohort. This analysis identified the aforementioned intronic variant in *PIK3CA* again. We also prioritized two intronic variants in *AFF2*, an intronic variant in *EPHA3*, and four intronic variants in *EXOC4*. All four genes were affected by a CNV in a single patient in the prior study. The *EPHA3* intronic variant is predicted to be pathogenic by EIGEN (0.58), to affect splicing,

and to fall within binding sites for CTCF, TCF12, and RAD21. All four *EXOC4* variants are predicted to affect splicing, and the *EXOC4* variant in intron 17 is predicted to be pathogenic by EIGEN (0.05) and GWAVA (0.5) and to fall within binding sites for GATA2 and GATA3.

Indels in prioritized genes

Finally, we investigated our cohort for rare, *de novo* indels affecting any of the 12 prioritized genes and identified two more variants: a 2-bp intronic deletion in *BCAS3* in Patient 20 and an intronic 8-bp insertion in *THBS2* in Patient 12, just upstream of the previously identified intronic SNV in *THBS2* in the same patient.

DECIPHER analyses

Next, we analyzed published CNVs using DECIPHER to identify previously reported individuals with a phenotypic description containing the term "hemangioma" and CNVs containing our prioritized genes. This analysis identified five individuals in DECIPHER with deletions affecting *THBS2*; a single individual each with a deletion affecting *BCAS3*, *GLRX3*, and *RASA3*; and a single individual each with a duplication affecting *DLC1* and *PIK3CA*.

We expanded our DECIPHER analysis to identify individuals with "facial hemangioma" and the genes disrupted by their CNVs. Next, we searched for rare, *de novo* variants in our cohort in the genes disrupted in two or more DECIPHER individuals. *THBS2* was only disrupted by deletions in DECIPHER. Another two genes were each disrupted by two CNVs, one deletion and one duplication, in DECIPHER individuals with facial hemangioma. *ALDH3A1* has a novel p.Val373Met variant in our Patient 8; this SNV is in the first codon of exon eight, is predicted to affect splicing by Human Splicing Finder (HSF), and is predicted to be

pathogenic by CADD (23.3) and FATHMM-MKL (0.48). *ATP7B* has a p.Thr482Ala variant in our Patient 10; this SNV is predicted to affect splicing by HSF.

We performed an enrichment analysis for the DECIPHER CNVs disrupting *ALDH3A1*, *ATP7B*, and *THBS2*. Only deletions disrupting *THBS2* were significantly more common among individuals with facial hemangioma (FET, p=3.7e-2, OR=7.17) or hemangioma (FET, p=3.9e-3, OR=5.24) in DECIPHER than among the individuals without these features in DECIPHER, respectively.

Pathway analysis

Genes containing rare, *de novo*, non-intergenic SNVs (n=4,320 genes) were analyzed through g:Profiler to look for common pathways disrupted in our cohort (Table 1). The five gene ontology (GO) terms with the most significant p-values were all related to development and morphogenesis. The most significant term, nervous system development (adjusted p=6.22e-24), included our candidate genes *AFF2*, *DLC1*, *EPHA3*, *PIK3CA*, and *THBS2*. We also observed an enrichment for cell adhesion (adjusted p=1.34e-10, including *BCAS3*, *DLC1*, *EPHA3*, *PIK3CA*, and *THBS2*), which is critical for angiogenesis. The three KEGG terms with the most significant p-values implicated RAP signaling (adjusted p=1.61e-6, including *PIK3CA*), focal adhesion (adjusted p=2.43e-6, including *PIK3CA* and *THBS2*), and phospholipase D signaling (adjusted p=8.13e-6, including *PIK3CA*).

Expression analysis

We explored the expression of the candidate genes *RASA3*, *AFF2*, *DLC1*, *EPHA3*, *PIK3CA*, and *THBS2* across diverse cell types in the human developing heart (Figure 2) by incorporating chromatin accessibility (scATAC-seq) (Ameen & Sundaram et. al.,

unpublished) and gene expression (scRNA-seq) datasets (Asp et al. 2019; Miao et al. 2020; Suryawanshi et al. 2020). We observed that *AFF2*, *EPHA3*, *PIK3CA*, and *THBS2* are co-expressed in the vasculature (pre-smooth muscle cells and vascular smooth muscle cells) in the fetal heart, whilst *AFF2*, *EPHA3*, and *PIK3CA* are co-expressed in the endothelium. Furthermore, *RASA3*, *DLC1*, and *THBS2* are co-expressed in pericytes, the mural cells surrounding blood vessels and embedded within the basement membrane of the vasculature and adjacent to endothelial cells (Armulik et al. 2005), and *RASA3* and *THBS2* are co-expressed in perivascular fibroblasts, which may serve as pericyte precursors (Rajan et al. 2020). Together, these data suggest that the expression of the candidate genes is enriched in endothelial cells and mural cells (pericytes and vascular smooth muscle cells) in the blood vessel wall.

DISCUSSION

Our whole genome sequencing analyses support a disruption in RAS pathway signaling as the primary pathogenic mechanism behind PHACE. The RAS pathway genes identified in our analysis are associated with abnormal angiogenesis, including changes to cytoskeletal organization, cell migration, and adhesion, in relevant knockout mouse models. DLC1 binds RASA1 (a paralog of RASA3) at focal adhesions, and *Dlc1* knockout causes embryonic lethal placenta vascular malformations (Durkin et al. 2005; Yang et al. 2009). EPHA3 regulates cytoskeletal organization, cell-cell adhesion, and cell migration in angiogenesis, and *Epha3* knockout causes perinatal lethal cardiac defects (Clifford et al. 2008; Vaidya et al. 2003; Vearing et al. 2005). PIK3CA regulates cell migration and adhesion and has been associated with vascular anomalies, and *Pik3ca* knockout causes embryonic lethal vascular defects and hemorrhage (Bi et al. 1999; Graupera et al. 2008; Lelievre et al. 2005). RASA3 regulates cell-cell and cell-matrix adhesion and cell

migration, and *Rasa3* knockout causes embryonic lethal hemorrhage following vascular lumenization defects (Iwashita et al. 2007; Molina-Ortiz et al. 2018). THBS2 binds heparin in the extracellular matrix (ECM), mediates cell-matrix interactions, and inhibits cell adhesion and angiogenesis, and *Thbs2* knockout causes increased vascularity and premature death (Bornstein et al. 2000; Kyriakides et al. 1998; Noh et al. 2003; Streit et al. 1999; Yang et al. 2000).

The g:Profiler pathway analysis of the genes with rare, *de novo* SNVs in these patients also implicated these same candidate genes. KEGG pathway analysis identified RAP signaling, focal adhesion, and phospholipase D (PLD) signaling as the most significantly affected pathways. RASA3 downregulates RAP1 GTPase signaling (Battram et al. 2017; Molina-Ortiz et al. 2018). BCAS3, DLC1, PIK3CA, and THBS2 all participate in the regulation of focal adhesion (Durkin et al. 2005; Elzie and Murphy-Ullrich 2004; Jain et al. 2012; Matsuoka et al. 2012; Yang et al. 2009). PLD is required for actin cytoskeleton remodeling in cell migration and angiogenesis, participates in RAS activation, and is activated by both RAS/MAPK/ERK and PI3K/AKT/mTOR signaling (Bruntz et al. 2014). RASA3 downregulates RAS signaling through MEK/ERK and also binds PI3K and regulates cell migration though PI3K-dependent integrin signaling (Battram et al. 2017; Castellano and Downward 2011). PIK3CA forms part of the PI3K complex and regulates endothelial cell migration during vascular development (Graupera et al. 2008). STAMBP binds GRB2 to regulate both the RAS/MAPK and PI3K/AKT/mTOR pathways (McDonell et al. 2013; Tsang et al. 2006). THBS2 signals through FAK activation of the MAPK/ERK and PI3K/AKT pathways to stimulate actin reorganization, decrease cell adhesion, and increase migration (Goicoechea et al. 2000; Greenwood et al. 1998; Orr et al. 2002). DLC1 and EPHA3 both bind RASA1, a close paralog of RASA3 (Haupaix et al. 2013; Yang et al. 2009); the *EPHA3* intronic variant in particular is also in a binding site for TCF12, which

downregulates ERK signaling (Yi et al. 2017). DLC1 is also phosphorylated by AKT, which abrogates its tumor suppression activity (Ko et al. 2010). The identification of variants in these genes among the probands with PHACE suggests that defects in matricellular signaling affecting endothelial cell adhesion and migration through the RAS and PI3K pathways may contribute to the pathogenesis of PHACE (Figure 3).

Our analysis of rare, *de novo* germline variants combined with the DECIPHER analysis of CNVs found in individuals with hemangioma identified *THBS2* as a strong candidate causative gene for PHACE. *THBS2* had missense and intronic variants in our cohort and was deleted in five individuals with hemangioma in DECIPHER; an enrichment analysis showed that deletions disrupting *THBS2* were significantly more common among individuals with hemangioma than in individuals without this feature in DECIPHER. While no human phenotype has been associated with this gene, knockout of this gene in a mouse causes blood vessel overgrowth and premature death (Bornstein et al. 2000; Kyriakides et al. 1998; Yang et al. 2000). *THBS2* is highly expressed in arterial tissues (aorta, coronary, and tibial) described in GTEx and in the developing vasculature in our scRNA analysis. THBS2 interacts with the ECM, mediates cell-matrix interactions, inhibits cell adhesion, inhibits angiogenesis, and acts as a tumor suppressor (Bornstein et al. 2000; Kyriakides et al. 1998; Noh et al. 2003; Streit et al. 1999; Yang et al. 2000). The *THBS2* residue p.Asp859, which had a missense variant in our cohort, is found in the C-terminal type 3 repeats and participates in calcium binding (Figure 1). This calcium binding is necessary for correct folding of the C terminus, which itself must correctly trimerize in order to support the integrin-binding and cell motility functions of the THBS2 protein (Anilkumar et al. 2002; Carlson et al. 2008; Kvansakul et al. 2004). Therefore, a variant in this position could affect the protein function by disrupting protein folding and trimerization.

Our analysis identified *RASA3* as a second strong candidate causative gene for PHACE. *RASA3* had a missense variant in our cohort and was deleted in one DECIPHER individual with capillary hemangioma. Germline pathogenic variants in a related gene, *RASA1*, are known to cause capillary malformation–arteriovenous malformation (Eerola et al. 2003). No human phenotype has been associated with *RASA3*, but knockout of this gene in a mouse causes hemorrhage and embryonic lethality due to vascular abnormalities (Iwashita et al. 2007; Molina-Ortiz et al. 2018). *RASA3* also regulates angiogenesis via the RAS/RAP pathway (Molina-Ortiz et al. 2018), which was implicated in our pathway analysis, and was highly expressed in pericytes in our scRNA analysis.

We also identified seven noncoding variants in four RAS pathway genes (*DLC1*, *EPHA3*, *PIK3CA*, and *THBS2*). These variants were predicted to affect splicing, functional DNA, transcription factor binding, and/or open chromatin in vascular cells (Table 2). The genes *DLC1* and *PIK3CA* are highly intolerant to loss-of-function coding mutations (probability of loss-of-function intolerance scores > 0.9) (Lek et al. 2016) and have enhanced expression in PHACE-relevant tissues: *DLC1* in neurons and retinal amacrine cells and *PIK3CA* in aorta and coronary artery (Genotype-Tissue Expression (GTEx) Project 2021). Single cell RNA expression analyses also showed that our candidate RAS pathway genes have high expression in neural crest, smooth muscle, and endothelial cells in the developing heart (Figure 2). The predicted disruption of expression and/or splicing of these genes by our identified noncoding variants may therefore contribute to other PHACE features. For instance, an intronic SNV, rs1905014-T, in *DLC1* is significantly associated with optic disc size (Han et al. 2019). However, the effects of the noncoding variants on splicing and/or functional DNA need to be investigated further.

In conclusion, we have found strong candidate coding and noncoding variants in genes in the RAS/MAPK and PI3K/AKT pathways in individual patients with PHACE. These variants, paired with the vascular birthmark (infantile hemangioma) and the structural brain, heart, arterial, and eye anomalies in PHACE, support the inclusion of PHACE as a RASopathy syndrome. It is striking that the majority of these variants were predicted to have effects that may lead to altered gene expression during development. However, because of the complex cellular interactions between vascular cell types, further *in vivo* studies are necessary to confirm pathogenicity of the variants identified and to understand their effect on the pathways that are likely disrupted by these variants.

SUBJECTS AND METHODS

Subjects

Patients with PHACE and their parents were recruited and sequenced as part of the Gabriella Miller Kids First Pediatric Research Program (X01HL140519-01). The study is approved by the Medical College of Wisconsin IRB #PRO00034867 and patients gave written, informed consent. Of the 98 patients discussed here, 19 were male, and 85 were white (Table 3). The average age of the cohort was 5.8 years at the time of enrollment. Ninety patients had facial hemangioma.

Germline whole genome sequencing and *de novo* analysis pipeline

WGS was performed on germline DNA from 98 unrelated patients with PHACE and their parents. WGS libraries were sequenced on the Illumina NovaSeq 6000 platform using 150-bp paired ends and the NovaSeq 6000 S4 Reagent Kit (Illumina, San Diego, California). Alignment was performed using DRAGEN (v.SW: 01.011.269.3.2.8) (Ma et al. 2015); data conversion from

CRAM to BAM files with samtools (v.1.9); data pre-processing with Picard RevertSam, MarkDuplicates, SortSam, and MergeBamAlignment (v2.18.2) (Broad Institute 2019) and base quality recalibration with GATK BQSR (v.4.0.3.0). Germline variant calling and single-sample gVCF generation were performed using GATK HaplotypeCaller (v.3.5-0-g36282e4). Genotype analysis of trios/families, *de novo* variant discovery, variant quality recalibration, joint variant calling on all samples, and recalculation of genotype call accuracy on the population level were performed with GATK tools (Van der Auwera et al. 2013): HaplotypeCaller (v.3.5-0-g36282e4), VariantAnnotator (v.3.8-0-ge9d806836), VQSR, CalculateGenotypePosteriors, and VariantFiltration (v.4.0.12.0). All outputs were released to the DRC Portal and dbGaP, where the files can be accessed and downloaded (github.com/kids-first/kf-alignment-workflow).

High confidence *de novo* SNVs and indels were called for variants present only in the proband with GQ scores ≥ 20 for all trio members. Resulting variants were lifted to GRCh37/hg19 using UCSC's liftOver tool and annotated using Annovar (v2013_09_11) (Wang et al. 2010). The liftover was necessary because the TraP and GWAVA annotations (see Variant prioritization) are not available under hg38.

Variant prioritization

Variants were subset to include SNVs with gnomAD (Karczewski et al. 2020) minor allele frequency (MAF) < 1% (hereafter defined as rare). Next, we prioritized SNVs that:

1) were not present in gnomAD (novel);

2) affected a gene already known to cause a phenotype overlapping that of PHACE in OMIM (omim.org) or GWAS annotation (Buniello et al. 2019);

3) affected a gene where the mouse model phenotype (informatics.jax.org) overlapped that of PHACE;

4) affected genes disrupted by CNVs described by Siegel et al. (2013); or

5) affected genes with coding variants in two or more patients.

Prioritized coding variants were further evaluated for pathogenicity prediction scores using VarSome (Kopanos et al. 2019).

Prioritized noncoding variants were further evaluated for scores designed to predict effects on splicing [TraP (Gelfman et al. 2017), Human Splicing Finder (HSF) (Desmet et al. 2009)]; functional DNA [CADD (Rentzsch et al. 2019), DANN (Quang et al. 2015), GWAVA (Ritchie et al. 2014), EIGEN (Ionita-Laza et al. 2016), FATHMM (Shihab et al. 2015)]; transcription factor binding sites (TFBS) (Euskirchen et al. 2007); and open chromatin in vascular cells in Encode (Ernst et al. 2011).

Finally, we investigated the *de novo* indels identified in the genes prioritized using metrics 1-5.

DECIPHER analyses

We first selected the pathogenic or likely pathogenic deletions and duplications described in DECIPHER (Firth et al. 2009) in individuals with hemangioma. We compared the genes affected by these CNVs with the genes prioritized in our cohort (described above) to identify other individuals in DECIPHER with hemangiomas and CNVs affecting our prioritized genes.

We then selected all pathogenic or likely pathogenic CNVs described in DECIPHER in individuals with facial hemangioma. The “facial hemangioma” feature was chosen to represent PHACE because it is the most common manifestation of this syndrome. We

identified 47 DECIPHER individuals with facial hemangioma, with a total of 55 CNVs (17 gains, 38 losses) disrupting 5,703 genes; 1,191 of these genes were disrupted in at least two DECIPHER individuals. This subset of 1,191 genes was compared to the list of rare, *de novo* variants identified in our cohort of patients with PHACE to prioritize further candidates.

An enrichment analysis was performed for each gene identified by the second DECIPHER analysis. The DECIPHER pathogenic or likely pathogenic deletions disrupting the gene of interest in individuals with facial hemangioma were classified as "cases". The DECIPHER pathogenic or likely pathogenic deletions disrupting the same gene in individuals without facial hemangioma were classified as "controls". For each gene we built a contingency table comparing the number of cases to controls and performed a Fisher's exact test (FET) using a cutoff of p-value < 0.05 for statistical significance. For significant genes we also calculated an odds ratio.

Sanger sequencing

Prioritized candidate variants were validated by Sanger sequencing. DNA from the proband and each parent was amplified using Accuprime Taq polymerase (Invitrogen; 12339-016) using standard thermal cycling conditions with annealing at 60˚C and variant-specific primer sequences (Supplemental Table 2). Small aliquots of each PCR product were run on a 1% agarose gel to verify amplification, and the remainder of each PCR product was cleaned up using a mixture of exonuclease 1 (Affymetrix; 70073X) and shrimp alkaline phosphatase (Affymetrix; 78390) and sequenced using the same primers.

Protein structure analysis

The experimentally derived structure of THBS2 was obtained from RCSB PDB (Berman et al. 2000) structure 1YO8 (Carlson et al. 2005). The effect of the identified p.Asp859Asn variant in THBS2 was examined using DynaMut (Rodrigues et al. 2018), which predicts the effects of missense mutations on known PDB structures.

Pathway analysis

All 4,320 genes with rare, *de novo* SNVs were analyzed with gProfiler (Raudvere et al. 2019) to determine if they had similar functions or affected the same pathways. Multiple testing-adjusted p-values (using the default g:SCS method in gProfiler) were reported, and 0.05 was used as the cutoff for statistical significance.

Expression analysis

The chromatin accessibility atlas and gene expression data of the human developing heart was derived from nuclei isolated from human fetal hearts (Ameen & Sundaram et al., *unpublished*). Briefly, the Chromium 10X platform (Satpathy et al. 2019) was used to generate scATAC-seq data from three primary human fetal heart samples at 6, 8, and 19 weeks post-gestation. The scRNA-seq data from fetal hearts were analyzed from published studies (Asp et al. 2019; Miao et al. 2020; Suryawanshi et al. 2020) using the batch correction algorithm Harmony (Korsunsky et al. 2019), and then annotated using known cell-type-specific marker genes.

DATA AVAILABILITY

Datasets related to this article are accessible through the Kids First Data Resource Portal (kidsfirstdrc.org) and/or dbGaP (ncbi.nlm.nih.gov/gap) accession phs001785.v1.p1.

ORCIDS

Elizabeth S. Partan: 0000-0002-3995-6742

Francine Blei: 0000-0001-6726-2361

Sarah L. Chamlin: 0000-0002-0845-2306

Olivia M. T. Davies: 0000-0001-5428-7279

Beth A. Drolet: 0000-0002-0844-7195

Ilona J. Frieden: 0000-0001-7305-5940

Ioannis Karakikes: 0000-0002-4348-600X

Chien-Wei Lin: 0000-0003-4023-7339

Anthony J. Mancini: 0000-0003-0903-7734

Denise Metry: 0000-0003-1991-1683

Anthony Oro: 0000-0002-6261-138X

Nicole S. Stefanko: 0000-0002-3609-3144

Laksshman Sundaram: 0000-0002-8953-3940

Monika Tutaj: 0000-0002-0378-4002

Alexander E. Urban: 0000-0001-9772-933X

Kevin C. Wang: 0000-0002-5305-6791

Xiaowei Zhu: 0000-0002-5731-3177

Nara Sobreira: 0000-0002-5228-5613

Dawn H. Siegel: 0000-0001-6546-2693

CONFLICT OF INTEREST

Francine Blei has received honoraria and non-drug related educational grants from Pierre Fabre. Sarah Chamlin is a speaker for Sanofi Genzyme and Regeneron Pharmaceuticals. Beth Drolet is a consultant and on the clinical advisory board for Venthera. Ilona Frieden serves on the Data Safety monitoring boards for Pfizer, is a consultant and advisory board member for Novartis, and is a consultant for Venthera. Dawn Siegel has received royalties from UpToDate, is a consultant for Arqule/Merck, and received a SID SUN mid-career investigator award.

ACKNOWLEDGMENTS

We thank all the families for their participation in this study, and the PHACE Syndrome Community and Pediatric Dermatology Research Alliance (PeDRA) for support of this project. We acknowledge the support of the Children's Research Institute at Children's Wisconsin and the Genomic Sciences and Precision Medicine Center at Medical College of Wisconsin.

The results analyzed and shown here are based in part upon data generated by Gabriella Miller Kids First Pediatric Research Program (Kids First) projects phs001785.v1.p1. Kids First was supported by the Common Fund of the Office of the Director of the

National Institutes of Health (commonfund.nih.gov/KidsFirst). The Hudson-Alpha Institute for Biotechnology was awarded a U24HD090744-01 to sequence structural birth defect cohort samples submitted by investigators through the Kids First program (1X01HL140519-01).

This study was supported by the NICHD, NHLBI, and NIAMS under award numbers 1X01HL14519, R03HD098526, and R01AR064258, respectively. The content is solely the responsibility of the authors and does not necessarily represent the official views of the National Institutes of Health. Additional support was received from a SID SUN grant, PHACE Foundation Canada, and the Children's Research Institute.

This study makes use of data generated by the DECIPHER community. A full list of centers who contributed to the generation of the data is available from decipher.sanger.ac.uk and via email from decipher@sanger.ac.uk. Funding for the project was provided by Wellcome. The individuals who carried out the original analysis and collection of the data bear no responsibility for the further analysis or interpretation of it in this paper.

AUTHOR CONTRIBUTIONS (CREDIT)

Elizabeth S. Partan: Conceptualization, Data curation, Investigation, Visualization, Writing – original draft, Writing – review & editing

Francine Blei: Data curation, Writing – review & editing

Sarah L. Chamlin: Data curation, Writing – review & editing

Olivia M. T. Davies: Data curation, Writing – review & editing

Beth A. Drolet: Data curation, Writing – review & editing

Ilona J. Frieden: Data curation, Writing – review & editing

Ioannis Karakikes: Writing – review & editing

Chien-Wei Lin: Formal analysis, Writing – review & editing

Anthony J. Mancini: Data curation, Writing – review & editing

Denise Metry: Data curation, Writing – review & editing

Anthony Oro: Writing – review & editing

Nicole S. Stefanko: Data curation, Writing – review & editing

Laksshman Sundaram: Investigation, Visualization

Monika Tutaj: Data curation, Formal analysis, Writing – review & editing

Alexander E. Urban: Writing – review & editing

Kevin C. Wang: Writing – review & editing

Xiaowei Zhu: Writing – review & editing

Nara Sobreira: Conceptualization, Funding acquisition, Project administration, Supervision, Writing – review & editing

Dawn H. Siegel: Conceptualization, Data curation, Funding acquisition, Project administration, Supervision, Writing – review & editing

REFERENCES

Anilkumar N, Annis DS, Mosher DF, Adams JC. Trimeric assembly of the C-terminal region of thrombospondin-1 or thrombospondin-2 is necessary for cell spreading and fascin spike organisation. J Cell Sci. The Company of Biologists Ltd; 2002;115(11):2357–66 Available from: https://jcs.biologists.org/content/115/11/2357

Armulik A, Abramsson A, Betsholtz C. Endothelial/pericyte interactions. Circulation Research. American Heart Association; 2005;97(6):512–23 Available from: http://www.ahajournals.org/doi/10.1161/01.RES.0000182903.16652.d7

Asp M, Giacomello S, Larsson L, Wu C, Fürth D, Qian X, et al. A spatiotemporal organ-wide gene expression and cell atlas of the developing human heart. Cell. 2019;179(7):1647-1660.e19 Available from: https://www.sciencedirect.com/science/article/pii/S0092867419312826

Battram AM, Durrant TN, Agbani EO, Heesom KJ, Paul DS, Piatt R, et al. The phosphatidylinositol 3,4,5-trisphosphate (PI(3,4,5)P3) binder Rasa3 regulates phosphoinositide 3-kinase (PI3K)-dependent integrin αIIbβ3 outside-in signaling. J Biol Chem. 2017;292(5):1691–704

Berman HM, Westbrook J, Feng Z, Gilliland G, Bhat TN, Weissig H, et al. The Protein Data Bank. Nucleic Acids Research. 2000;28(1):235–42 Available from: https://doi.org/10.1093/nar/28.1.235

Bi L, Okabe I, Bernard DJ, Wynshaw-Boris A, Nussbaum RL. Proliferative defect and embryonic lethality in mice homozygous for a deletion in the p110α subunit of phosphoinositide 3-kinase. J. Biol. Chem. American Society for Biochemistry and Molecular Biology; 1999;274(16):10963–8 Available from: http://www.jbc.org/content/274/16/10963

Bornstein P, Kyriakides TR, Yang Z, Armstrong LC, Birk DE. Thrombospondin 2 modulates collagen fibrillogenesis and angiogenesis. Journal of Investigative Dermatology Symposium Proceedings. 2000;5(1):61–6 Available from: http://www.sciencedirect.com/science/article/pii/S0022202X15528601

Broad Institute. Picard Toolkit [Internet]. Broad Institute, GitHub Repository; 2019. Available from: http://broadinstitute.github.io/picard/

Bruntz RC, Lindsley CW, Brown HA. Phospholipase D signaling pathways and phosphatidic acid as therapeutic targets in cancer. Pharmacol Rev. 2014;66(4):1033–79 Available from: https://www.ncbi.nlm.nih.gov/pmc/articles/PMC4180337/

Buniello A, MacArthur JAL, Cerezo M, Harris LW, Hayhurst J, Malangone C, et al. The NHGRI-EBI GWAS Catalog of published genome-wide association studies, targeted arrays and summary statistics 2019. Nucleic Acids Res. 2019;47(D1):D1005–12

Carlson CB, Bernstein DA, Annis DS, Misenheimer TM, Hannah BA, Mosher DF, et al. Structure of the calcium-rich signature domain of human thrombospondin-2. Nat Struct Mol Biol. 2005;12(10):910–4 Available from: http://www.nature.com/articles/nsmb997

Carlson CB, Gunderson KA, Mosher DF. Mutations targeting intermodular interfaces or calcium binding destabilize the thrombospondin-2 signature domain. J Biol Chem. 2008;283(40):27089–99 Available from: https://www.ncbi.nlm.nih.gov/pmc/articles/PMC2555992/

Castellano E, Downward J. RAS interaction with PI3K. Genes Cancer. 2011;2(3):261–74 Available from: https://www.ncbi.nlm.nih.gov/pmc/articles/PMC3128635/

Chacon□Camacho OF, Lopez□Moreno D, Morales□Sanchez MA, Hofmann E, Pacheco□Quito M, Wieland I, et al. Expansion of the phenotypic spectrum and description of molecular findings in a cohort of patients with oculocutaneous mosaic RASopathies. Mol Genet Genomic Med. 2019;7(5):e625 Available from: https://www.ncbi.nlm.nih.gov/pmc/articles/PMC6503218/

Clifford N, Smith LM, Powell J, Gattenlöhner S, Marx A, O'Connor R. The EphA3 receptor is expressed in a subset of rhabdomyosarcoma cell lines and suppresses cell adhesion and migration. Journal of Cellular Biochemistry. 2008;105(5):1250–9 Available from: http://onlinelibrary.wiley.com/doi/abs/10.1002/jcb.21926

Desmet F-O, Hamroun D, Lalande M, Collod-Béroud G, Claustres M, Béroud C. Human Splicing Finder: An online bioinformatics tool to predict splicing signals. Nucleic Acids Res. 2009;37(9):e67

Durkin ME, Avner MR, Huh C-G, Yuan B-Z, Thorgeirsson SS, Popescu NC. DLC-1, a Rho GTPase-activating protein with tumor suppressor function, is essential for embryonic development. FEBS Letters. 2005;579(5):1191–6 Available from: http://www.sciencedirect.com/science/article/pii/S001457930500089X

Eerola I, Boon LM, Mulliken JB, Burrows PE, Dompmartin A, Watanabe S, et al. Capillary malformation–arteriovenous malformation, a new clinical and genetic disorder caused by RASA1 mutations. The American Journal of Human Genetics. Elsevier; 2003;73(6):1240–9 Available from: https://www.cell.com/ajhg/abstract/S0002-9297(07)63977-9

Elzie CA, Murphy-Ullrich JE. The N-terminus of thrombospondin: The domain stands apart. The International Journal of Biochemistry & Cell Biology. 2004;36(6):1090–101 Available from: http://www.sciencedirect.com/science/article/pii/S1357272503004357

Ernst J, Kheradpour P, Mikkelsen TS, Shoresh N, Ward LD, Epstein CB, et al. Mapping and analysis of chromatin state dynamics in nine human cell types. Nature. 2011;473(7345):43–9 Available from: https://www.ncbi.nlm.nih.gov/pmc/articles/PMC3088773/

Euskirchen GM, Rozowsky JS, Wei C-L, Lee WH, Zhang ZD, Hartman S, et al. Mapping of transcription factor binding regions in mammalian cells by ChIP: Comparison of array- and sequencing-based technologies. Genome Res. 2007;17(6):898–909

Firth HV, Richards SM, Bevan AP, Clayton S, Corpas M, Rajan D, et al. DECIPHER: Database of Chromosomal Imbalance and Phenotype in Humans Using Ensembl Resources. Am J Hum Genet. 2009;84(4):524–33 Available from: https://www.ncbi.nlm.nih.gov/pmc/articles/PMC2667985/

Frieden IJ, Reese V, Cohen D. PHACE syndrome: The association of posterior fossa brain malformations, hemangiomas, arterial anomalies, coarctation of the aorta and cardiac defects, and eye abnormalities. Arch Dermatol. 1996;132(3):307–11 Available from: https://jamanetwork.com/journals/jamadermatology/fullarticle/557585

Garzon MC, Epstein LG, Heyer GL, Frommelt PC, Orbach DB, Baylis AL, et al. PHACE syndrome: Consensus-derived diagnosis and care recommendations. The Journal of Pediatrics. 2016;178:24-33.e2 Available from: https://www.jpeds.com/article/S0022-3476(16)30656-4/fulltext

Gelfman S, Wang Q, McSweeney KM, Ren Z, La Carpia F, Halvorsen M, et al. Annotating pathogenic non-coding variants in genic regions. Nature Communications. 2017;8(1):236 Available from: http://www.nature.com/articles/s41467-017-00141-2

Genotype-Tissue Expression (GTEx) Project. GTEx portal [Internet]. 2021 [cited 2021 Jun 22]. Available from: https://www.gtexportal.org/home/

Goicoechea S, Orr AW, Pallero MA, Eggleton P, Murphy-Ullrich JE. Thrombospondin mediates focal adhesion disassembly through interactions with cell surface calreticulin. J. Biol. Chem. American Society for Biochemistry and Molecular Biology; 2000;275(46):36358–68 Available from: http://www.jbc.org/content/275/46/36358

Grant AR, Cushman BJ, Cavé H, Dillon MW, Gelb BD, Gripp KW, et al. Assessing the gene–disease association of 19 genes with the RASopathies using the ClinGen gene curation framework. Hum Mutat. 2018;39(11):1485–93 Available from: https://www.ncbi.nlm.nih.gov/pmc/articles/PMC6326381/

Graupera M, Guillermet-Guibert J, Foukas LC, Phng L-K, Cain RJ, Salpekar A, et al. Angiogenesis selectively requires the p110α isoform of PI3K to control endothelial cell migration. Nature. Nature Publishing Group; 2008;453(7195):662–6 Available from: https://www.nature.com/articles/nature06892

Greenwood JA, Pallero MA, Theibert AB, Murphy-Ullrich JE. Thrombospondin signaling of focal adhesion disassembly requires activation of phosphoinositide 3-kinase. J. Biol. Chem. American Society for Biochemistry and Molecular Biology; 1998;273(3):1755–63 Available from: http://www.jbc.org/content/273/3/1755

Han X, Qassim A, An J, Marshall H, Zhou T, Ong J-S, et al. Genome-wide association analysis of 95,549 individuals identifies novel loci and genes influencing optic disc morphology. Hum Mol Genet. 2019;28(21):3680–90

Haupaix N, Stolfi A, Sirour C, Picco V, Levine M, Christiaen L, et al. p120RasGAP mediates ephrin/Eph-dependent attenuation of FGF/ERK signals during cell fate specification in ascidian embryos. Development. 2013;140(21):4347–52

Hopkin RJ, Schorry E, Bofinger M, Milatovich A, Stern HJ, Jayne C, et al. New insights into the phenotypes of 6q deletions. American Journal of Medical Genetics. 1997;70(4):377–86 Available from: http://onlinelibrary.wiley.com/doi/abs/10.1002/%28SICI%291096-8628%2819970627%2970%3A4%3C377%3A%3AAID-AJMG9%3E3.0.CO%3B2-Q

Ionita-Laza I, McCallum K, Xu B, Buxbaum JD. A spectral approach integrating functional genomic annotations for coding and noncoding variants. Nat. Genet. 2016;48(2):214–20

Ishii N, Owada Y, Yamada M, Miura S, Murata K, Asao H, et al. Loss of neurons in the hippocampus and cerebral cortex of AMSH-deficient mice. Mol Cell Biol. 2001;21(24):8626–37

Iwashita S, Kobayashi M, Kubo Y, Hinohara Y, Sezaki M, Nakamura K, et al. Versatile roles of R-Ras GAP in neurite formation of PC12 cells and embryonic vascular development. J. Biol. Chem. American Society for Biochemistry and Molecular Biology; 2007;282(6):3413–7 Available from: http://www.jbc.org/content/282/6/3413

Jain M, Bhat GP, VijayRaghavan K, Inamdar MS. Rudhira/BCAS3 is a cytoskeletal protein that controls Cdc42 activation and directional cell migration during angiogenesis. Experimental Cell Research. 2012;318(6):753–67 Available from: http://www.sciencedirect.com/science/article/pii/S0014482712000377

Karczewski KJ, Francioli LC, Tiao G, Cummings BB, Alföldi J, Wang Q, et al. The mutational constraint spectrum quantified from variation in 141,456 humans. Nature. Nature Publishing Group; 2020;581(7809):434–43 Available from: https://www.nature.com/articles/s41586-020-2308-7

Kinsler VA, Thomas AC, Ishida M, Bulstrode NW, Loughlin S, Hing S, et al. Multiple congenital melanocytic nevi and neurocutaneous melanosis are caused by postzygotic mutations in codon 61 of NRAS. J Invest Dermatol. 2013;133(9):2229–36 Available from: https://www.ncbi.nlm.nih.gov/pmc/articles/PMC3678977/

Ko FCF, Chan L, Tung EK, Lowe SW, Ng IO, Yam JWP. Akt phosphorylation of Deleted in Liver Cancer 1 abrogates its suppression of liver cancer tumorigenesis and metastasis. Gastroenterology. 2010;139(4):1397-1407.e6 Available from: https://www.sciencedirect.com/science/article/pii/S0016508510009601

Kopanos C, Tsiolkas V, Kouris A, Chapple CE, Albarca Aguilera M, Meyer R, et al. VarSome: The human genomic variant search engine. Bioinformatics. 2019;35(11):1978–80 Available from: https://doi.org/10.1093/bioinformatics/bty897

Korsunsky I, Millard N, Fan J, Slowikowski K, Zhang F, Wei K, et al. Fast, sensitive, and accurate integration of single cell data with Harmony. Nat Methods. 2019;16(12):1289–96 Available from: https://www.ncbi.nlm.nih.gov/pmc/articles/PMC6884693/

Kvansakul M, Adams JC, Hohenester E. Structure of a thrombospondin C-terminal fragment reveals a novel calcium core in the type 3 repeats. The EMBO Journal. John Wiley & Sons, Ltd; 2004;23(6):1223–33 Available from: https://www.embopress.org/doi/full/10.1038/sj.emboj.7600166

Kyriakides TR, Zhu Y-H, Smith LT, Bain SD, Yang Z, Lin MT, et al. Mice that lack thrombospondin 2 display connective tissue abnormalities that are associated with disordered collagen fibrillogenesis, an increased vascular density, and a bleeding diathesis. Journal of Cell Biology. 1998;140(2):419–30 Available from: https://doi.org/10.1083/jcb.140.2.419

Lek M, Karczewski KJ, Minikel EV, Samocha KE, Banks E, Fennell T, et al. Analysis of protein-coding genetic variation in 60,706 humans. Nature. 2016;536(7616):285–91 Available from: https://www.nature.com/articles/nature19057

Lelievre E, Bourbon P-M, Duan L-J, Nussbaum RL, Fong G-H. Deficiency in the p110α subunit of PI3K results in diminished Tie2 expression and Tie2-/–like vascular defects in mice. Blood. 2005;105(10):3935–8 Available from: https://www.ncbi.nlm.nih.gov/pmc/articles/PMC1895075/

Ma S, Jiang T, Jiang R. Differential regulation enrichment analysis via the integration of transcriptional regulatory network and gene expression data. Bioinformatics. 2015;31(4):563–71

Martel C, Robertson R, Williams FB, Moore RC, Clark A. Anesthetic management of a parturient with PHACE syndrome for cesarean delivery. A&A Practice. 2015;5(10):176–8 Available from: https://journals.lww.com/aacr/subjects/Cardiovascular/Fulltext/2015/11150/Anesthetic_Management_of_a_Parturient_with_PHACE.3.aspx

Matsuoka T, Yashiro M, Nishioka N, Hirakawa K, Olden K, Roberts JD. PI3K/Akt signalling is required for the attachment and spreading, and growth in vivo of metastatic scirrhous gastric carcinoma. British Journal of Cancer. Nature Publishing Group; 2012;106(9):1535–42 Available from: https://www.nature.com/articles/bjc2012107

McDonell LM, Mirzaa GM, Alcantara D, Schwartzentruber J, Carter MT, Lee LJ, et al. Mutations in STAMBP, encoding a deubiquitinating enzyme, cause Microcephaly-Capillary Malformation syndrome. Nat Genet. 2013;45(5):556–62 Available from: https://www.ncbi.nlm.nih.gov/pmc/articles/PMC4000253/

Metry DW, Haggstrom AN, Drolet BA, Baselga E, Chamlin S, Garzon M, et al. A prospective study of PHACE syndrome in infantile hemangiomas: Demographic features, clinical findings, and complications. American Journal of Medical Genetics Part A. 2006;140A(9):975–86 Available from: https://onlinelibrary.wiley.com/doi/abs/10.1002/ajmg.a.31189

Metry DW, Heyer G, Hess C, Garzon M, Haggstrom A, Frommelt P, et al. Consensus statement on diagnostic criteria for PHACE syndrome. Pediatrics. 2009;124(5):1447–56 Available from: http://pediatrics.aappublications.org/content/124/5/1447

Miao Y, Tian L, Martin M, Paige SL, Galdos FX, Li J, et al. Intrinsic endocardial defects contribute to hypoplastic left heart syndrome. Cell Stem Cell. 2020;27(4):574-589.e8 Available from: https://www.sciencedirect.com/science/article/pii/S1934590920303532

Mitchell S, Siegel DH, Shieh JTC, Stevenson DA, Grimmer JF, Lewis T, et al. Candidate locus analysis for PHACE syndrome. Am. J. Med. Genet. A. 2012;158A(6):1363–7

Molina-Ortiz P, Orban T, Martin M, Habets A, Dequiedt F, Schurmans S. Rasa3 controls turnover of endothelial cell adhesion and vascular lumen integrity by a Rap1-dependent mechanism. PLOS Genetics. Public Library of Science; 2018;14(1):e1007195 Available from: https://journals.plos.org/plosgenetics/article?id=10.1371/journal.pgen.1007195

Noh Y-H, Matsuda K, Hong Y-K, Kunstfeld R, Riccardi L, Koch M, et al. An N-terminal 80 kDa recombinant fragment of human thrombospondin-2 inhibits vascular endothelial growth factor induced endothelial cell migration in vitro and tumor growth and angiogenesis in vivo. Journal of Investigative Dermatology. 2003;121(6):1536–43 Available from: http://www.sciencedirect.com/science/article/pii/S0022202X15305637

Orr AW, Pallero MA, Murphy-Ullrich JE. Thrombospondin stimulates focal adhesion disassembly through Gi- and phosphoinositide 3-kinase-dependent ERK activation. Journal of Biological Chemistry. 2002;277(23):20453–60 Available from: http://www.sciencedirect.com/science/article/pii/S0021925820848881

Peeden JN, Scarbrough P, Taysi K, Wilroy RS, Finley S, Luthardt F, et al. Ring chromosome 6: Variability in phenotypic expression. Am J Med Genet. 1983;16(4):563–73

Petit P, Fryns JP, van den Berghe H. Partial trisomy 13 with phenotype of Patau syndrome due to maternal reciprocal translocation t(6;13)(q25;q13). Ann Genet. 1980;23(1):57–9

Quang D, Chen Y, Xie X. DANN: A deep learning approach for annotating the pathogenicity of genetic variants. Bioinformatics. 2015;31(5):761–3

Rajan AM, Ma RC, Kocha KM, Zhang DJ, Huang P. Dual function of perivascular fibroblasts in vascular stabilization in zebrafish. PLOS Genetics. Public Library of Science; 2020;16(10):e1008800 Available from: https://journals.plos.org/plosgenetics/article?id=10.1371/journal.pgen.1008800

Raudvere U, Kolberg L, Kuzmin I, Arak T, Adler P, Peterson H, et al. g:Profiler: A web server for functional enrichment analysis and conversions of gene lists (2019 update). Nucleic Acids Res. Oxford Academic; 2019;47(W1):W191–8 Available from: https://academic.oup.com/nar/article/47/W1/W191/5486750

Rentzsch P, Witten D, Cooper GM, Shendure J, Kircher M. CADD: Predicting the deleteriousness of variants throughout the human genome. Nucleic Acids Res. 2019;47(D1):D886–94

Ritchie GRS, Dunham I, Zeggini E, Flicek P. Functional annotation of noncoding sequence variants. Nat Methods. Nature Publishing Group; 2014;11(3):294–6 Available from: https://www.nature.com/articles/nmeth.2832

Rodrigues CH, Pires DE, Ascher DB. DynaMut: Predicting the impact of mutations on protein conformation, flexibility and stability. Nucleic Acids Res. 2018;46(Web Server issue):W350–5 Available from: https://www.ncbi.nlm.nih.gov/pmc/articles/PMC6031064/

Römke C, Heyne K, Stewens J, Schwinger E. Erroneous diagnosis of fetal alcohol syndrome in a patient with ring chromosome 6. Eur J Pediatr. 1987;146(4):443

Ruggieri M, Polizzi A, Marceca GP, Catanzaro S, Praticò AD, Di Rocco C. Introduction to phacomatoses (neurocutaneous disorders) in childhood. Childs Nerv Syst. 2020;36(10):2229–68 Available from: https://doi.org/10.1007/s00381-020-04758-5

Satpathy AT, Granja JM, Yost KE, Qi Y, Meschi F, McDermott GP, et al. Massively parallel single-cell chromatin landscapes of human immune cell development and intratumoral T cell exhaustion. Nat Biotechnol. 2019;37(8):925–36 Available from: https://www.ncbi.nlm.nih.gov/pmc/articles/PMC7299161/

Shihab HA, Rogers MF, Gough J, Mort M, Cooper DN, Day INM, et al. An integrative approach to predicting the functional effects of non-coding and coding sequence variation. Bioinformatics. 2015;31(10):1536–43

Siegel DH. PHACE syndrome [Internet]. UpToDate. 2017. Available from: https://www.uptodate.com/contents/phace-syndrome

Siegel DH, Shieh JTC, Kwon E-K, Baselga E, Blei F, Cordisco M, et al. Copy number variation analysis in 98 individuals with PHACE syndrome. J. Invest. Dermatol. 2013;133(3):677–84

Stefanko NS, Cossio M-L, Powell J, Blei F, Davies OMT, Frieden IJ, et al. Natural history of PHACE syndrome: A survey of adults with PHACE. Pediatric Dermatology. 2019;36(5):618–22 Available from: http://onlinelibrary.wiley.com/doi/abs/10.1111/pde.13871

Stevenson DA, Schill L, Schoyer L, Andresen BS, Bakker A, Bayrak-Toydemir P, et al. The Fourth International Symposium on Genetic Disorders of the Ras/MAPK pathway. Am J Med Genet A. 2016;170(8):1959–66 Available from: https://www.ncbi.nlm.nih.gov/pmc/articles/PMC4945362/

Streit M, Riccardi L, Velasco P, Brown LF, Hawighorst T, Bornstein P, et al. Thrombospondin-2: A potent endogenous inhibitor of tumor growth and angiogenesis. PNAS. National Academy of Sciences; 1999;96(26):14888–93 Available from: https://www.pnas.org/content/96/26/14888

Suryawanshi H, Clancy R, Morozov P, Halushka MK, Buyon JP, Tuschl T. Cell atlas of the foetal human heart and implications for autoimmune-mediated congenital heart block. Cardiovasc Res. 2020;116(8):1446–57 Available from: https://www.ncbi.nlm.nih.gov/pmc/articles/PMC7314636/

Tsang HTH, Connell JW, Brown SE, Thompson A, Reid E, Sanderson CM. A systematic analysis of human CHMP protein interactions: Additional MIT domain-containing proteins bind to multiple components of the human ESCRT III complex. Genomics. 2006;88(3):333–46 Available from: http://www.sciencedirect.com/science/article/pii/S0888754306001121

Vaidya A, Pniak A, Lemke G, Brown A. EphA3 null mutants do not demonstrate motor axon guidance defects. Mol Cell Biol. 2003;23(22):8092–8 Available from: https://www.ncbi.nlm.nih.gov/pmc/articles/PMC262425/

Van der Auwera GA, Carneiro MO, Hartl C, Poplin R, del Angel G, Levy□Moonshine A, et al. From FASTQ data to high-confidence variant calls: The Genome Analysis Toolkit best practices pipeline. Current Protocols in Bioinformatics. 2013;43(1):11.10.1-11.10.33 Available from: http://currentprotocols.onlinelibrary.wiley.com/doi/abs/10.1002/0471250953.bi1110s43

Vearing C, Lee F-T, Wimmer-Kleikamp S, Spirkoska V, To C, Stylianou C, et al. Concurrent binding of anti-EphA3 antibody and ephrin-A5 amplifies EphA3 signaling and downstream responses: Potential as EphA3-specific tumor-targeting reagents. Cancer Res. American Association for Cancer Research; 2005;65(15):6745–54 Available from: https://cancerres.aacrjournals.org/content/65/15/6745

Wan J, Steiner J, Baselga E, Blei F, Cordisco MR, Garzon MC, et al. Prenatal risk factors for PHACE syndrome: A study using the PHACE syndrome international clinical registry and genetic repository. The Journal of Pediatrics. 2017;190:275–9 Available from: https://www.sciencedirect.com/science/article/pii/S0022347617309058

Wang K, Li M, Hakonarson H. ANNOVAR: Functional annotation of genetic variants from high-throughput sequencing data. Nucleic Acids Res. Oxford Academic; 2010;38(16):e164–e164 Available from: https://academic.oup.com/nar/article/38/16/e164/1749458

Yang X-Y, Guan M, Vigil D, Der CJ, Lowy DR, Popescu NC. p120Ras-GAP binds the DLC1 Rho-GAP tumor suppressor protein and inhibits its RhoA GTPase and growth-suppressing activities. Oncogene. 2009;28(11):1401–9

Yang Z, Kyriakides TR, Bornstein P. Matricellular proteins as modulators of cell-matrix interactions: Adhesive defect in thrombospondin 2-null fibroblasts is a consequence of increased levels of matrix metalloproteinase-2. Mol Biol Cell. 2000;11(10):3353–64

Yi S, Yu M, Yang S, Miron RJ, Zhang Y. Tcf12, a member of basic helix-loop-helix transcription factors, mediates bone marrow mesenchymal stem cell osteogenic differentiation in vitro and in vivo. Stem Cells. 2017;35(2):386–97

TABLES

Table 1: g:Profiler pathway analysis of genes with rare, *de novo* variants

A) Gene ontology (GO) terms

Term ID	Term name	Adjusted p-value	# genes
GO:0007399	nervous system development	6.22E-24	646
GO:0000902	cell morphogenesis	1.88E-23	329
GO:0032989	cellular component morphogenesis	6.85E-20	260
GO:0048666	neuron development	8.51E-20	343
GO:0032990	cell part morphogenesis	1.15E-19	236
GO:0016043	cellular component organization	1.84E-19	1413
GO:0031175	neuron projection development	4.82E-19	309
GO:0030182	neuron differentiation	5.53E-19	401
GO:0120039	plasma membrane bounded cell projection morphogenesis	6.95E-19	228
GO:0120036	plasma membrane bounded cell projection organization	1.54E-18	428
GO:0048858	cell projection morphogenesis	1.60E-18	228
GO:0048812	neuron projection morphogenesis	2.63E-18	223
GO:0048699	generation of neurons	1.10E-17	433
GO:0030030	cell projection organization	2.90E-17	432
GO:0071840	cellular component organization or biogenesis	7.38E-17	1432
GO:0043167	ion binding	1.10E-16	1378
GO:0048468	cell development	1.23E-16	563
GO:0000904	cell morphogenesis involved in differentiation	1.31E-16	239
GO:0022008	neurogenesis	4.92E-16	449
GO:0048667	cell morphogenesis involved in neuron differentiation	3.46E-15	199
GO:0051128	regulation of cellular component organization	6.13E-15	599
GO:0019899	enzyme binding	9.62E-15	566
GO:0010975	regulation of neuron projection development	1.34E-14	176
GO:0034330	cell junction organization	4.11E-14	217
GO:0048856	anatomical structure development	5.63E-14	1312
GO:0051960	regulation of nervous system development	6.34E-14	280
GO:0120035	regulation of plasma membrane bounded cell projection organization	8.37E-14	217
GO:0031344	regulation of cell projection organization	2.28E-13	218
GO:0007275	multicellular organism development	4.63E-13	1211
GO:0045664	regulation of neuron differentiation	6.17E-13	211
GO:0022604	regulation of cell morphogenesis	6.51E-13	166

Term ID	Term name	Adjusted p-value	# genes
GO:0009653	anatomical structure morphogenesis	7.53E-13	669
GO:0048731	system development	5.70E-12	1101
GO:0032502	developmental process	5.86E-12	1397
GO:0043168	anion binding	4.70E-11	666
GO:0007264	small GTPase mediated signal transduction	9.61E-11	162
GO:0050767	regulation of neurogenesis	1.28E-10	243
GO:0007155	cell adhesion	1.34E-10	375
GO:0034329	cell junction assembly	1.51E-10	142
GO:0022610	biological adhesion	1.70E-10	376
GO:0060284	regulation of cell development	2.17E-10	273
GO:0051130	positive regulation of cellular component organization	3.48E-10	320
GO:0016358	dendrite development	4.05E-10	94
GO:0023051	regulation of signaling	4.09E-10	820
GO:0046872	metal ion binding	1.06E-09	930
GO:0051056	regulation of small GTPase mediated signal transduction	1.09E-09	112
GO:0007010	cytoskeleton organization	1.28E-09	356
GO:0050839	cell adhesion molecule binding	1.78E-09	163
GO:0065008	regulation of biological quality	2.06E-09	899
GO:0030029	actin filament-based process	2.57E-09	226
GO:0010769	regulation of cell morphogenesis involved in differentiation	3.24E-09	108
GO:0010646	regulation of cell communication	3.33E-09	806
GO:0043169	cation binding	3.43E-09	943
GO:0050773	regulation of dendrite development	3.93E-09	66
GO:0050808	synapse organization	6.33E-09	133
GO:0007409	axonogenesis	6.46E-09	150
GO:0006996	organelle organization	9.75E-09	877
GO:0032559	adenyl ribonucleotide binding	1.99E-08	383
GO:0031346	positive regulation of cell projection organization	2.79E-08	127
GO:0030554	adenyl nucleotide binding	4.80E-08	383
GO:0051020	GTPase binding	5.13E-08	162
GO:0019904	protein domain specific binding	5.21E-08	198
GO:0044093	positive regulation of molecular function	5.34E-08	436
GO:0005524	ATP binding	6.16E-08	368
GO:0030036	actin cytoskeleton organization	6.68E-08	198
GO:0061564	axon development	8.00E-08	157
GO:0010976	positive regulation of neuron projection development	8.83E-08	100
GO:0051962	positive regulation of nervous system development	9.77E-08	165

Term ID	Term name	Adjusted p-value	# genes
GO:0099536	synaptic signaling	1.00E-07	200
GO:0007169	transmembrane receptor protein tyrosine kinase signaling pathway	2.31E-07	207
GO:0017016	Ras GTPase binding	2.65E-07	127
GO:0099537	trans-synaptic signaling	3.45E-07	193
GO:0097367	carbohydrate derivative binding	4.49E-07	521
GO:0051179	localization	4.95E-07	1402
GO:0031267	small GTPase binding	5.62E-07	129
GO:0005085	guanyl-nucleotide exchange factor activity	7.05E-07	78
GO:0008092	cytoskeletal protein binding	7.54E-07	252
GO:0035556	intracellular signal transduction	8.74E-07	632
GO:0022607	cellular component assembly	9.90E-07	658
GO:0032879	regulation of localization	1.04E-06	643
GO:0030165	PDZ domain binding	1.11E-06	40
GO:0045666	positive regulation of neuron differentiation	1.32E-06	120
GO:0043087	regulation of GTPase activity	1.85E-06	141
GO:0048522	positive regulation of cellular process	2.05E-06	1190
GO:0044087	regulation of cellular component biogenesis	2.11E-06	252
GO:0097485	neuron projection guidance	2.18E-06	94
GO:0098916	anterograde trans-synaptic signaling	2.20E-06	188
GO:0007268	chemical synaptic transmission	2.20E-06	188
GO:0007416	synapse assembly	2.75E-06	67
GO:0140096	catalytic activity, acting on a protein	2.88E-06	512
GO:0032553	ribonucleotide binding	3.02E-06	446
GO:0005088	Ras guanyl-nucleotide exchange factor activity	3.18E-06	48
GO:0032555	purine ribonucleotide binding	3.67E-06	442
GO:0007411	axon guidance	4.05E-06	93
GO:0043085	positive regulation of catalytic activity	4.06E-06	352
GO:0050804	modulation of chemical synaptic transmission	4.09E-06	125
GO:0005509	calcium ion binding	4.56E-06	191
GO:0099177	regulation of trans-synaptic signaling	4.80E-06	125
GO:0017076	purine nucleotide binding	5.98E-06	443
GO:0005515	protein binding	6.42E-06	2726
GO:0004672	protein kinase activity	7.71E-06	163
GO:0005543	phospholipid binding	8.46E-06	130
GO:0016773	phosphotransferase activity, alcohol group as acceptor	8.79E-06	186
GO:0048813	dendrite morphogenesis	1.23E-05	57
GO:0008047	enzyme activator activity	1.41E-05	146

Term ID	Term name	Adjusted p-value	# genes
GO:0009966	regulation of signal transduction	1.45E-05	697
GO:0006928	movement of cell or subcellular component	1.72E-05	514
GO:0035639	purine ribonucleoside triphosphate binding	1.78E-05	424
GO:0007417	central nervous system development	2.20E-05	263
GO:0003779	actin binding	2.23E-05	125
GO:0004674	protein serine/threonine kinase activity	2.32E-05	127
GO:1900006	positive regulation of dendrite development	2.51E-05	35
GO:0000166	nucleotide binding	2.83E-05	486
GO:1901265	nucleoside phosphate binding	3.01E-05	486
GO:0007167	enzyme linked receptor protein signaling pathway	3.04E-05	270
GO:0050769	positive regulation of neurogenesis	4.05E-05	140
GO:0050770	regulation of axonogenesis	4.21E-05	66
GO:0003824	catalytic activity	4.34E-05	1198
GO:1901888	regulation of cell junction assembly	4.39E-05	68
GO:0006793	phosphorus metabolic process	4.54E-05	731
GO:0050807	regulation of synapse organization	5.70E-05	72
GO:0060589	nucleoside-triphosphatase regulator activity	6.63E-05	102
GO:0007420	brain development	6.98E-05	201
GO:0006796	phosphate-containing compound metabolic process	7.81E-05	724
GO:0043547	positive regulation of GTPase activity	8.09E-05	118
GO:0007015	actin filament organization	8.49E-05	125
GO:0031589	cell-substrate adhesion	8.93E-05	107
GO:0016301	kinase activity	9.70E-05	204
GO:0050803	regulation of synapse structure or activity	1.07E-04	74
GO:0017124	SH3 domain binding	1.17E-04	48
GO:0099173	postsynapse organization	1.31E-04	56
GO:0036094	small molecule binding	1.59E-04	562
GO:0099003	vesicle-mediated transport in synapse	2.05E-04	64
GO:0007265	Ras protein signal transduction	2.14E-04	102
GO:0065009	regulation of molecular function	2.14E-04	658
GO:0033036	macromolecule localization	2.22E-04	689
GO:0016772	transferase activity, transferring phosphorus-containing groups	2.31E-04	235
GO:0032535	regulation of cellular component size	2.34E-04	112
GO:0060322	head development	2.38E-04	208
GO:0030695	GTPase regulator activity	2.70E-04	91
GO:0007267	cell-cell signaling	3.04E-04	407
GO:0046578	regulation of Ras protein signal transduction	3.20E-04	65

Term ID	Term name	Adjusted p-value	# genes
GO:0010720	positive regulation of cell development	3.53E-04	155
GO:0005096	GTPase activator activity	3.71E-04	83
GO:0007215	glutamate receptor signaling pathway	3.83E-04	41
GO:0032501	multicellular organismal process	4.13E-04	1568
GO:0048638	regulation of developmental growth	4.16E-04	104
GO:0044085	cellular component biogenesis	4.75E-04	683
GO:0008289	lipid binding	4.80E-04	194
GO:0005089	Rho guanyl-nucleotide exchange factor activity	4.82E-04	27
GO:0098609	cell-cell adhesion	4.87E-04	218
GO:0099504	synaptic vesicle cycle	6.06E-04	60
GO:0031325	positive regulation of cellular metabolic process	6.53E-04	728
GO:0048518	positive regulation of biological process	6.85E-04	1278
GO:0007610	behavior	6.94E-04	160
GO:0010770	positive regulation of cell morphogenesis involved in differentiation	7.11E-04	55
GO:0035091	phosphatidylinositol binding	7.32E-04	78
GO:0050793	regulation of developmental process	7.36E-04	605
GO:0090066	regulation of anatomical structure size	7.48E-04	142
GO:0019900	kinase binding	7.78E-04	188
GO:0008104	protein localization	8.26E-04	609
GO:0018193	peptidyl-amino acid modification	8.42E-04	305
GO:0044089	positive regulation of cellular component biogenesis	8.53E-04	147
GO:0051239	regulation of multicellular organismal process	8.55E-04	721
GO:0061572	actin filament bundle organization	9.13E-04	56
GO:0033043	regulation of organelle organization	9.80E-04	306
GO:0050790	regulation of catalytic activity	1.10E-03	520
GO:0019901	protein kinase binding	1.14E-03	169
GO:0051173	positive regulation of nitrogen compound metabolic process	1.16E-03	690
GO:0016740	transferase activity	1.27E-03	513
GO:0003013	circulatory system process	1.33E-03	166
GO:0040011	locomotion	1.60E-03	444
GO:0036211	protein modification process	1.61E-03	876
GO:0006464	cellular protein modification process	1.61E-03	876
GO:0097435	supramolecular fiber organization	1.78E-03	182
GO:2000026	regulation of multicellular organismal development	1.78E-03	491
GO:0048583	regulation of response to stimulus	1.79E-03	899
GO:0005178	integrin binding	1.82E-03	50
GO:0051963	regulation of synapse assembly	1.92E-03	39

Term ID	Term name	Adjusted p-value	# genes
GO:0051049	regulation of transport	2.04E-03	417
GO:0030154	cell differentiation	2.20E-03	896
GO:0048869	cellular developmental process	2.20E-03	911
GO:0048589	developmental growth	2.26E-03	173
GO:0048588	developmental cell growth	2.26E-03	74
GO:0033674	positive regulation of kinase activity	2.57E-03	158
GO:0051234	establishment of localization	2.59E-03	1089
GO:0006468	protein phosphorylation	2.63E-03	447
GO:0051017	actin filament bundle assembly	2.76E-03	54
GO:0051345	positive regulation of hydrolase activity	2.94E-03	191
GO:0042391	regulation of membrane potential	2.96E-03	121
GO:0022603	regulation of anatomical structure morphogenesis	3.22E-03	282
GO:0008361	regulation of cell size	3.28E-03	60
GO:0016310	phosphorylation	3.46E-03	535
GO:0005488	binding	3.68E-03	3124
GO:0009893	positive regulation of metabolic process	3.71E-03	815
GO:1990138	neuron projection extension	4.17E-03	57
GO:0010604	positive regulation of macromolecule metabolic process	4.40E-03	757
GO:0098742	cell-cell adhesion via plasma-membrane adhesion molecules	4.54E-03	81
GO:0046873	metal ion transmembrane transporter activity	4.71E-03	116
GO:0006935	chemotaxis	5.27E-03	165
GO:0051641	cellular localization	5.39E-03	722
GO:0031646	positive regulation of nervous system process	5.44E-03	28
GO:0032970	regulation of actin filament-based process	5.97E-03	112
GO:0042330	taxis	6.39E-03	165
GO:0034220	ion transmembrane transport	6.77E-03	272
GO:0015020	glucuronosyltransferase activity	6.93E-03	17
GO:0019902	phosphatase binding	7.35E-03	60
GO:0044260	cellular macromolecule metabolic process	7.38E-03	1639
GO:0060627	regulation of vesicle-mediated transport	7.97E-03	140
GO:0048814	regulation of dendrite morphogenesis	8.38E-03	36
GO:0048041	focal adhesion assembly	8.46E-03	33
GO:0048639	positive regulation of developmental growth	8.67E-03	60
GO:0051094	positive regulation of developmental process	8.79E-03	334
GO:0051493	regulation of cytoskeleton organization	9.17E-03	144
GO:0048013	ephrin receptor signaling pathway	9.39E-03	34
GO:0044877	protein-containing complex binding	9.50E-03	287

Term ID	Term name	Adjusted p-value	# genes
GO:0042578	phosphoric ester hydrolase activity	9.92E-03	102
GO:0048523	negative regulation of cellular process	1.00E-02	1019
GO:1902414	protein localization to cell junction	1.02E-02	39
GO:0010810	regulation of cell-substrate adhesion	1.03E-02	66
GO:0034332	adherens junction organization	1.12E-02	28
GO:0017048	Rho GTPase binding	1.12E-02	51
GO:0060341	regulation of cellular localization	1.22E-02	235
GO:0004115	3',5'-cyclic-AMP phosphodiesterase activity	1.29E-02	9
GO:0023056	positive regulation of signaling	1.33E-02	417
GO:0006810	transport	1.63E-02	1056
GO:1990782	protein tyrosine kinase binding	1.68E-02	35
GO:0007156	homophilic cell adhesion via plasma membrane adhesion molecules	1.77E-02	54
GO:0051347	positive regulation of transferase activity	1.84E-02	171
GO:0010771	negative regulation of cell morphogenesis involved in differentiation	1.92E-02	36
GO:0052696	flavonoid glucuronidation	1.95E-02	8
GO:0034765	regulation of ion transmembrane transport	2.01E-02	128
GO:0007160	cell-matrix adhesion	2.08E-02	69
GO:0043412	macromolecule modification	2.14E-02	904
GO:0010647	positive regulation of cell communication	2.19E-02	414
GO:0060560	developmental growth involved in morphogenesis	2.21E-02	71
GO:0040007	growth	2.34E-02	233
GO:0008015	blood circulation	2.35E-02	142
GO:0099175	regulation of postsynapse organization	2.36E-02	35
GO:0006836	neurotransmitter transport	2.49E-02	65
GO:0008081	phosphoric diester hydrolase activity	2.54E-02	33
GO:0032956	regulation of actin cytoskeleton organization	2.88E-02	99
GO:0040008	regulation of growth	3.00E-02	169
GO:0007044	cell-substrate junction assembly	3.23E-02	36
GO:0051258	protein polymerization	3.42E-02	84
GO:0061387	regulation of extent of cell growth	3.55E-02	39
GO:0004114	3',5'-cyclic-nucleotide phosphodiesterase activity	3.61E-02	14
GO:0008066	glutamate receptor activity	3.61E-02	14
GO:0071495	cellular response to endogenous stimulus	3.93E-02	317
GO:1902903	regulation of supramolecular fiber organization	4.07E-02	101
GO:0045296	cadherin binding	4.16E-02	88
GO:0016049	cell growth	4.29E-02	126
GO:0045665	negative regulation of neuron differentiation	4.29E-02	67

Term ID	Term name	Adjusted p-value	# genes
GO:0150115	cell-substrate junction organization	4.30E-02	37
GO:0008038	neuron recognition	4.33E-02	22
GO:0051336	regulation of hydrolase activity	4.41E-02	292
GO:0017137	Rab GTPase binding	4.43E-02	52
GO:0030010	establishment of cell polarity	4.50E-02	46
GO:0005201	extracellular matrix structural constituent	4.60E-02	51
GO:0051640	organelle localization	4.69E-02	160
GO:0045595	regulation of cell differentiation	4.95E-02	423

B) KEGG pathways

Term ID	Term name	Adjusted p-value	# genes
KEGG:04015	Rap1 signaling pathway	1.61E-06	72
KEGG:04510	focal adhesion	2.43E-06	69
KEGG:04072	phospholipase D signaling pathway	8.13E-06	54
KEGG:04360	axon guidance	1.38E-05	62
KEGG:04724	glutamatergic synapse	2.67E-05	44
KEGG:04935	growth hormone synthesis, secretion and action	8.32E-05	44
KEGG:05032	morphine addiction	8.98E-05	36
KEGG:04211	longevity regulating pathway	2.05E-04	35
KEGG:04213	longevity regulating pathway - multiple species	2.81E-04	27
KEGG:04810	regulation of actin cytoskeleton	3.47E-04	66
KEGG:04976	bile secretion	3.78E-04	35
KEGG:04012	ErbB signaling pathway	5.57E-04	33
KEGG:04512	ECM-receptor interaction	6.19E-04	34
KEGG:04151	PI3K-Akt signaling pathway	9.34E-04	97
KEGG:04022	cGMP-PKG signaling pathway	1.23E-03	53
KEGG:04728	dopaminergic synapse	2.00E-03	44
KEGG:01522	endocrine resistance	2.03E-03	35
KEGG:04611	platelet activation	2.46E-03	42
KEGG:04725	cholinergic synapse	2.98E-03	39
KEGG:04928	parathyroid hormone synthesis, secretion and action	3.61E-03	37
KEGG:04540	gap junction	4.93E-03	32
KEGG:04730	long-term depression	5.70E-03	24
KEGG:04713	circadian entrainment	6.84E-03	34
KEGG:04020	calcium signaling pathway	6.91E-03	59
KEGG:04911	insulin secretion	7.87E-03	31

Term ID	Term name	Adjusted p-value	# genes
KEGG:04926	relaxin signaling pathway	1.31E-02	41
KEGG:05100	bacterial invasion of epithelial cells	1.40E-02	27
KEGG:05412	arrhythmogenic right ventricular cardiomyopathy	1.48E-02	28
KEGG:04915	estrogen signaling pathway	1.52E-02	43
KEGG:04720	long-term potentiation	2.12E-02	25
KEGG:04520	adherens junction	2.25E-02	26
KEGG:04723	retrograde endocannabinoid signaling	2.43E-02	45
KEGG:04971	gastric acid secretion	3.04E-02	27
KEGG:04062	chemokine signaling pathway	4.03E-02	54
KEGG:04070	phosphatidylinositol signaling system	4.05E-02	32
KEGG:04912	GnRH signaling pathway	4.07E-02	31
KEGG:04925	aldosterone synthesis and secretion	4.99E-02	32

Table 2: Candidate germline *de novo* variants in RAS pathway genes

Gene	Patient ID	Patient phenotype	Variant (hg38)	Variant consequence	gnomAD MAF	Predicted effect on splicing?	Damaging functional DNA scores?	TFBS?	Open chromatin in HUVECs?	OMIM phenotype	Homozygous knockout mouse model	CNV(s)
DLC1	Patient 1	Infantile hemangioma; Cerebellar hypoplasia; Migration anomaly of cortex; Middle cerebral artery hypoplasia; Chorio-retinal coloboma	8:13089422: C:T	intronic SNV (intron 15)	1.9e-3	—	—	—	transcriptional elongation	colorectal cancer, somatic	neural tube, heart, brain, and vascular placenta defects; embryonic lethality[1]	1 duplication in DECIPHER [ID: 395935]
	Patient 17	Infantile hemangioma; Coarctation of aorta; Sternal pit	8:13104433: G:A	intronic SNV (intron 7)	novel	—	EIGEN=0.25	—	transcriptional elongation			
	Patient 3	Infantile hemangioma; Internal carotid artery hypoplasia; Internal carotid artery tortuosity; Absent vertebral artery; Tortuous aorta with pseudo-coarctation	8:13253055: G:C	intronic SNV (intron 5)	novel	HSF: activates cryptic acceptor site	—	—	strong enhancer			
EPHA3	Patient 9	Infantile hemangioma; Sternal cleft; Dental enamel defects	3:89246570: G:A	intronic SNV (intron 3)	novel	HSF: activates cryptic acceptor site, changes exonic splicing silencer / enhancer	EIGEN=0.58	CTCF, TCF12, RAD21	—	—	perinatal death due to cardiac failure[2]	1 duplication in PHACE
PIK3CA	Patient 5	Infantile hemangioma; Subglottic hemangioma; Supra-umbilical raphe	3:179200365: T:G	intronic SNV (intron 3)	novel	HSF: changes exonic splicing silencer / enhancer	EIGEN=0.21	—	weakly transcribed	CLAPO syndrome, somatic; CLOVE syndrome, somatic; Cowden syndrome; keratosis, seborrheic, somatic; macrodactyly, somatic; megalencephaly-capillary malformation-polymicrogyria syndrome, somatic; nevus, epidermal, somatic; variety of cancers, somatic	vascular defects; hemorrhage; growth retardation; embryonic lethality[3]	1 duplication in PHACE; 1 duplication in DECIPHER [ID: 283584]

[1] (Durkin et al. 2005)
[2] (Vaidya et al. 2003)
[3] (Bi et al. 1999; Graupera et al. 2008; Lelievre et al. 2005)

Gene	Patient ID	Patient phenotype	Variant (hg38)	Variant consequence	gnomAD MAF	Predicted effect on splicing?	Damaging functional DNA scores?	TFBS?	Open chromatin in HUVECs?	OMIM phenotype	Homozygous knockout mouse model	CNV(s)
RASA3	Patient 4	Hypoplasia of cerebellum; Infantile hemangioma; Internal carotid artery hypoplasia; Internal carotid artery tortuosity; Optic nerve dysplasia	13:114041023: C:T	p.Val85Met	1.2e-5	HSF: changes exonic splicing silencer / enhancer	CADD=23.6; FATHMM=0.95; GWAVA=0.44	—	transcriptional elongation	—	hemorrhage; embryonic lethality[4]	1 deletion in DECIPHER [ID: 393047]
STAMBP	Patient 16	Infantile hemangioma; Abnormal cerebral arterial morphology; Ventricular septal defect (VSD); Dental enamel hypoplasia	2:73850410: T:A	p.Ile301Asn	novel	—	CADD=27.7; FATHMM=0.99	—	weakly transcribed	microcephaly-capillary malformation syndrome	postnatal growth retardation; limb-clasping; hypocellular cerebral cortex; loss of hippocampal neurons; blepharoptosis; death of starvation at weaning[5]	—
THBS2	Patient 14	Infantile hemangioma; Absent left internal carotid artery	6:169225343: C:T	p.Asp589Asn	novel	—	CADD=28.4; FATHMM=0.96	—	—	—	blood vessel abnormalities; premature death[6]	5 deletions in DECIPHER [IDs: 392300[7], 392970[8], 392995[9], 396392[10], 402744]
	Patient 12	Infantile hemangioma; Aberrant right subclavian artery; Fetal origin of cerebral artery; Internal carotid artery hypoplasia; Internal carotid artery tortuosity; Vertebral artery hypoplasia; Apical muscular VSD	6:169243142:C: CCACATTCT	intronic 8-bp insertion (intron 5)	novel	—	—	IKZF1	—			
			6:169243176: C:T	intronic SNV (intron 5)	3.3e-5	—	FATHMM=0.41	IKZF1	—			

[4] (Iwashita et al. 2007)
[5] (Ishii et al. 2001)
[6] (Kyriakides et al. 1998)
[7] (Peeden et al. 1983)
[8] (Römke et al. 1987)
[9] (Petit et al. 1980)
[10] (Hopkin et al. 1997)

Table 3: Patient demographics

	Number of patients
Gender	
• Female	79
• Male	19
Race	
• White	85
• Black or African American	4
• Asian	2
• American Indian or Alaska Native	2
• Other or Unknown	5
Ethnicity	
• Not Hispanic or Latino	88
• Hispanic or Latino	10
Facial hemangioma	90
Age (average)	5.8 years

FIGURE LEGENDS

Figure 1: Location and consequences of *THBS2*–p.Asp859Asn variant

A) The location and interactions of p.Asp859 in the THBS2 protein structure 1YO8 in PDB. The p.Asp859 amino acid is highlighted in green. The surrounding amino acids that participate in hydrogen binding with p.Asp859 and/or coordination with the calcium ions are labeled. **B-C)** The wild-type **(B)** and mutant **(C)** structure predictions from DynaMut are given. The affected amino acid is highlighted in teal. Red dashes indicate hydrogen bonds, and orange dashes indicate weak hydrogen bonds. The p.Asp859Asn variant disrupts many of the interactions of p.Asp859 with its neighboring amino acids.

Figure 2: Expression of candidate genes in the developing heart at single cell level

A-F) Clustering of single cells by Uniform Manifold Approximation and Projection (UMAP) based on the differentially accessibility of open chromatin regions (scATAC-seq). Gene expression levels of *RASA3* **(A)**, *DLC1* **(B)**, *AFF2* **(C)**, *EPHA3* **(D)**, *PIK3CA* **(E)**, and *THBS2* **(F)** imputed from gene accessibility scores (scATAC-seq) and RNA expression (scRNA-seq). Annotation shows the expression level of each gene in the corresponding cell type cluster.

Figure 3: Diagram of proposed RAS signaling pathway

RAS is activated downstream of growth factor binding to cellular receptors, which signal through GRB2/SOS/STAMBP, and deactivated by RAS-GAP proteins (RASA1, RASA3), which interact with EPHA3 and DLC1. Activated RAS-GTP signals through the MEK/ERK and PI3K/AKT/mTOR pathways to upregulate cell growth, cell migration, and angiogenesis. PI3K is also activated through extracellular matrix (ECM) signaling: THBS2 binds to the ECM and to integrins, which link the cell to the ECM, and THBS2 signals through focal adhesion kinase (FAK) to PI3K. Protein names denoted with an asterisk (DLC1, EPHA3, PIK3CA, RASA3, STAMBP, THBS2) were found to have *de novo* variants in our cohort. Image created using BioRender.

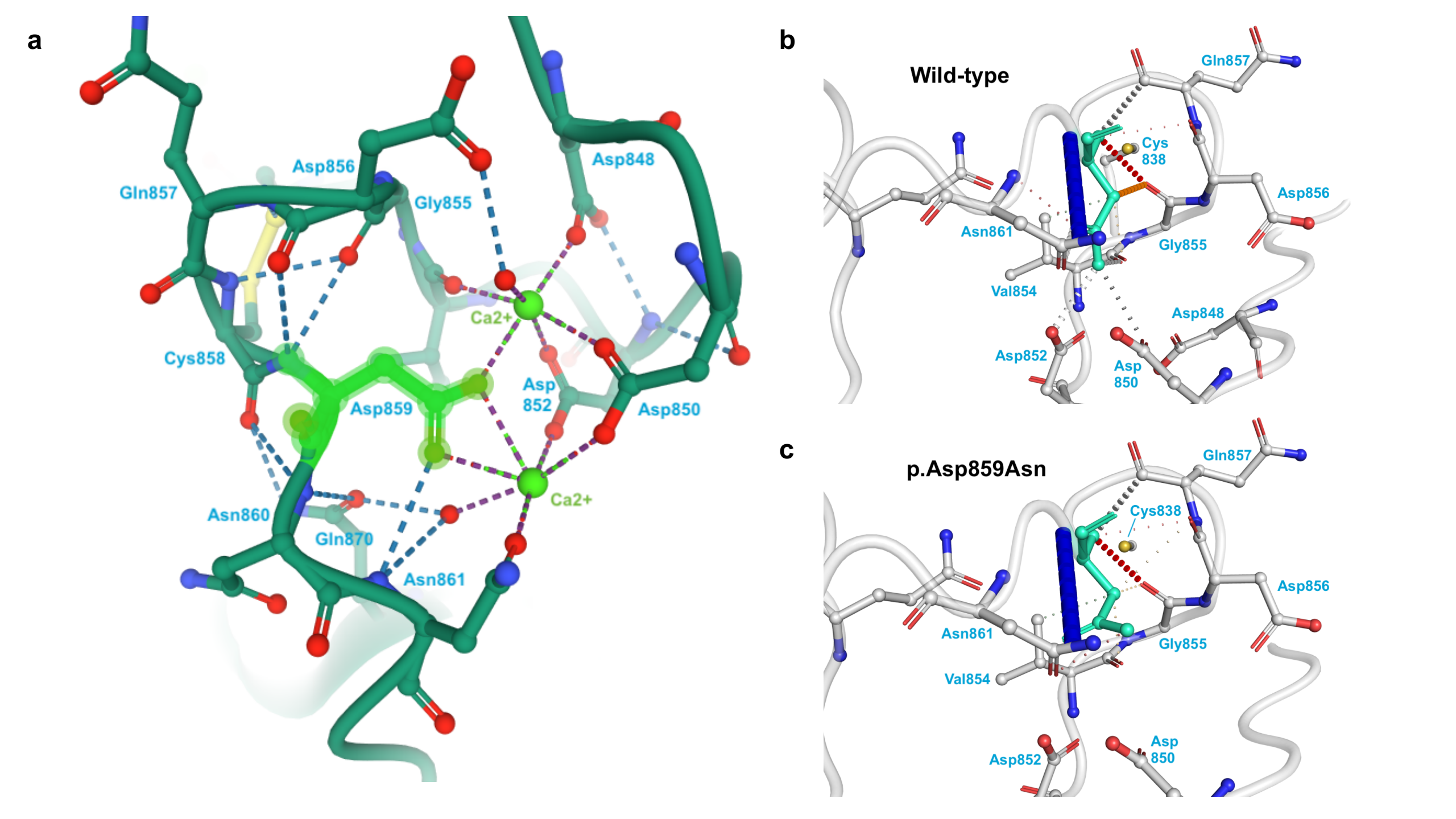
a
Asp856
Gln857
Gly855
Asp848
Ca2+
Cys858
Asp859
Asp
852
Asp850
Asn860
Gln870
Ca2+
Asn861
b
Wild-type
Gln857
Cys
838
Asp856
Asn861
Gly855
Val854
Asp848
Asp852
Asp
850
c
p.Asp859Asn
Gln857
Cys838
Asp856
Asn861
Gly855
Val854
Asp852
Asp
850

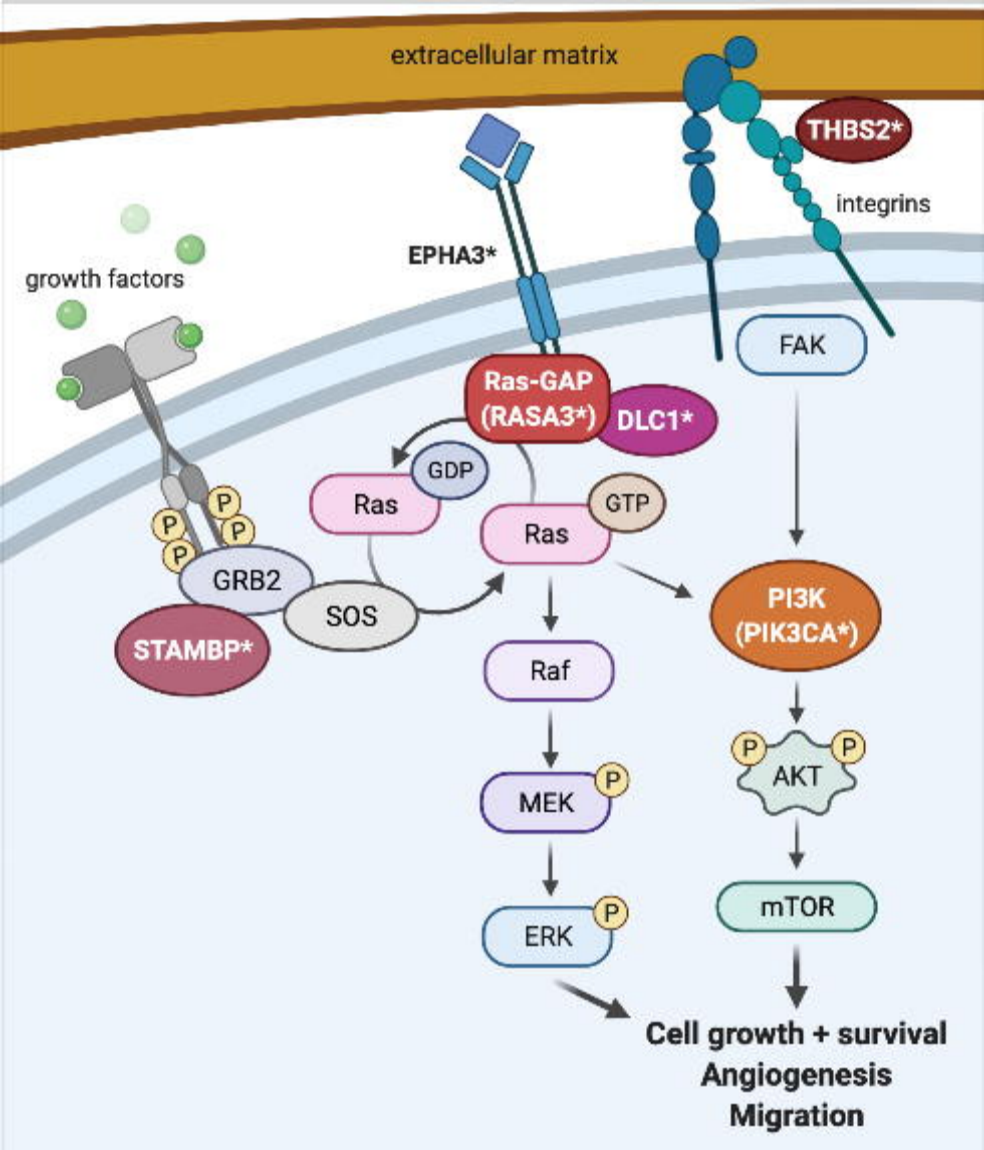
extracellular matrix
THBS2*
integrins
EPHA3*
growth factors
FAK
Ras-GAP
(RASA3*)
DLC1*
GDP
Ras
GTP
Ras
P
P
P
P
GRB2
SOS
STAMBP*
Raf
PI3K
(PIK3CA*)
MEK
P
P
AKT
P
ERK
P
mTOR
Cell growth + survival
Angiogenesis
Migration

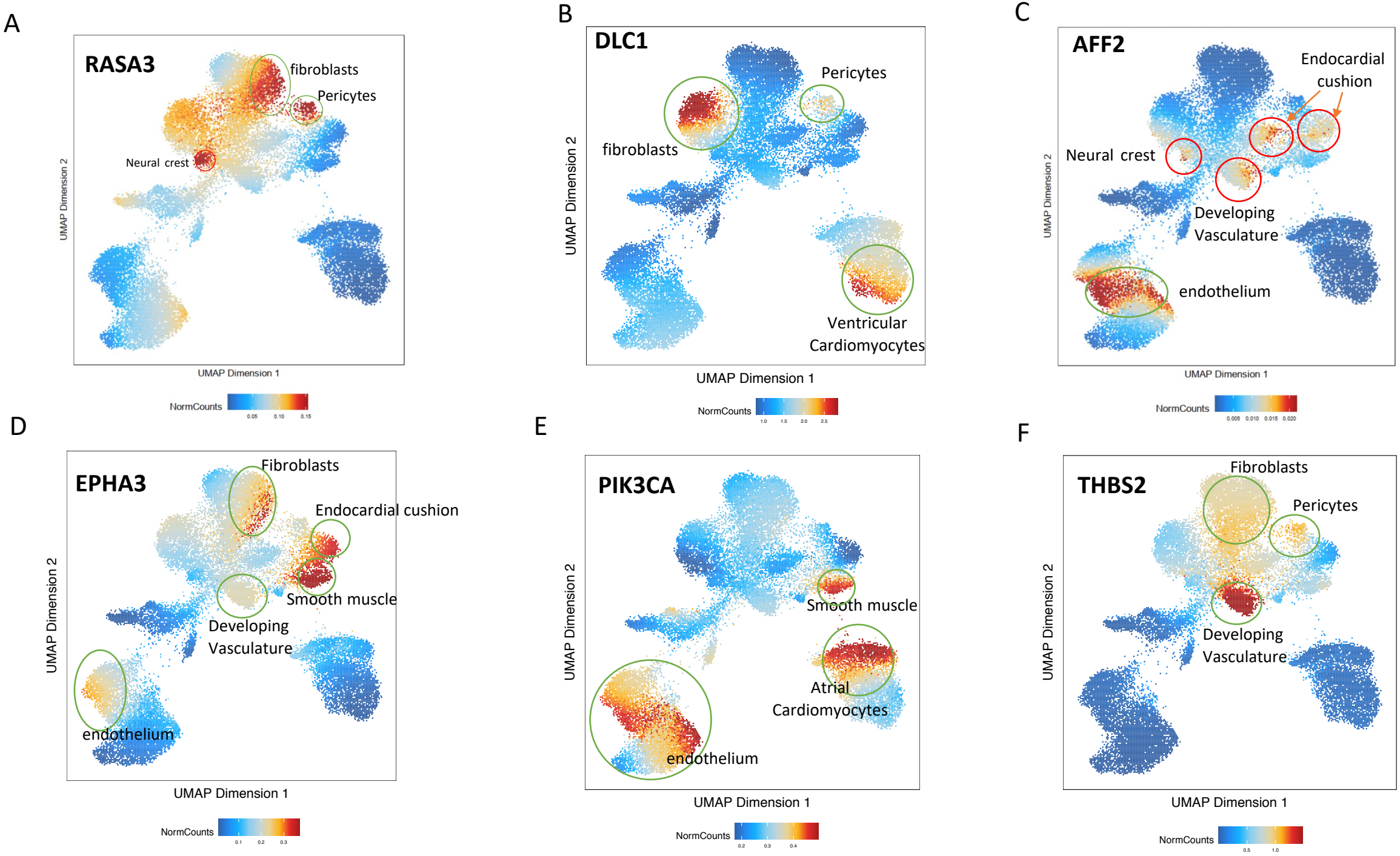
A
RASA3
fibroblasts
Pericytes
Neural crest
UMAP Dimension 2
UMAP Dimension 1
NormCounts
0.05
0.10
0.15
B
DLC1
Pericytes
fibroblasts
Ventricular
Cardiomyocytes
UMAP Dimension 2
UMAP Dimension 1
NormCounts
1.0
1.5
2.0
2.5
C
AFF2
Endocardial
cushion
Neural crest
Developing
Vasculature
endothelium
UMAP Dimension 2
UMAP Dimension 1
NormCounts
0.005
0.010
0.015
0.020
D
EPHA3
Fibroblasts
Endocardial cushion
Smooth muscle
Developing
Vasculature
endothelium
UMAP Dimension 2
UMAP Dimension 1
NormCounts
0.1
0.2
0.3
E
PIK3CA
Smooth muscle
Atrial
Cardiomyocytes
endothelium
UMAP Dimension 2
UMAP Dimension 1
NormCounts
0.2
0.3
0.4
F
THBS2
Fibroblasts
Pericytes
Developing
Vasculature
UMAP Dimension 2
UMAP Dimension 1
NormCounts
0.5
1.0